Impaired IFNγ responsiveness of monocyte-derived lung cells limits immunity to *Mycobacterium tuberculosis*

Weihao Zheng[1,*], Jason D. Limberis[1], Zachary P. Howard[1], Alexander Mohapatra[1], Enzo Takagi[2], Joel D. Ernst[1,*]

1 Division of Experimental Medicine, Department of Medicine, University of California, San Francisco, California, USA

2 Division of Nephrology, Department of Medicine, University of California, San Francisco, California, USA

*Correspondence: weihao.zheng@ucsf.edu (W.Z.), joel.ernst@ucsf.edu (J.D.E.)

Abstract

Lung mononuclear phagocyte (MNP) subsets differ in their ability to restrict *Mycobacterium tuberculosis* (Mtb) during chronic infection, yet the mechanisms underlying this difference are not well defined. Here, we show that CD11c^{lo} monocyte-derived cells (MNC1), the subset of lung cells that is most permissive for Mtb viability during chronic infection, express lower levels of interferon-gamma (IFNγ) signaling proteins, resulting in reduced responses to IFNγ compared to alveolar macrophages (AM) and CD11c^{hi} MNC2. Moreover, type I IFN signaling suppresses IFNγ-mediated MHC-II expression, impairing antigen-specific CD4 T cell activation by MNC1 cells. Importantly, prior immunity conferred by contained Mtb infection enhances IFNγ responsiveness of monocyte-derived cells, reducing bacterial burdens in lungs and within MNC subsets. Our findings indicate that heterogeneous IFNγ responsiveness is exploited by Mtb for persistence in vivo. Overcoming or bypassing impaired IFNγ responsiveness may guide the development of more effective TB vaccines and host-directed therapies.

Introduction

Tuberculosis (TB), caused by the respiratory pathogen *Mycobacterium tuberculosis* (Mtb), returned to being the leading cause of death from a single infectious disease worldwide as the COVID-19 pandemic subsided. It is imperative to identify mechanisms of immune protection and pathogenesis in TB to facilitate the development of novel TB vaccines and therapies.

Mtb is known for its ability to evade elimination by immune responses and cause chronic infection[1–3]. Multiple studies, including recent single-cell RNA sequencing studies, have revealed significant heterogeneity among lung mononuclear phagocytes (MNP) during Mtb infection[4–6]. Moreover, mounting evidence has established that Mtb infects multiple lung MNP subsets, among them, monocyte-derived cells (MNC) serve as the major bacterial reservoir during chronic infection[4,7–10]. After development of adaptive immune responses, distinct lung MNP subsets differ in Mtb-killing ability. Specifically, alveolar macrophages (AM) have a superior ability to restrict Mtb compared to monocyte-derived MNC1 and MNC2 cells [4,8]. Among these MNP subsets, CD11c^{lo} MNC1 is the most Mtb-permissive subset as defined by the number of live Mtb per infected cell, suggesting that functional heterogeneity of MNP contributes to Mtb persistence in vivo. We previously discovered heterogeneous lysosome function in these MNP subsets and found that in MNC1, lysosome deficiency is one cell type-specific host mechanism that contributes to Mtb persistence in vivo[8]. However, the mechanisms underlying the functional heterogeneity, particularly the differential ability of lung MNP subsets to respond to immune signals, remain incompletely defined.

Interferon-gamma (IFNγ) plays a critical role in host defense against Mtb, as evidenced by both human and murine studies[11–15]. Individuals with mutations in genes responsible for IFNγ immunity (e.g., *Ifng*, *Ifngr1*, *Ifngr2*, and *Stat1*) are susceptible to mycobacterial infections, including non-tuberculous mycobacteria and Mtb[11,16]. Studies utilizing knockout mice have demonstrated that both IFNγ and its receptor, IFNGR1, are essential for controlling Mtb infection, suggesting that the host's ability to produce IFNγ or to respond to IFNγ is required for IFNγ-mediated protection against TB[12–14]. Both hematopoietic and nonhematopoietic IFNγ responsiveness are required for Mtb control[14]. Paradoxically, TB vaccines that predominantly induce IFNγ often fail to enhance lung protection[1]. Moreover, murine studies indicate that increasing IFNγ production does not enhance Mtb control in the lungs, suggesting that cellular responsiveness to IFNγ may be a key determinant of its efficacy [17]. It remains unknown whether distinct lung MNP subsets differ in their ability to sense and transduce IFNγ signals during primary Mtb infection, and whether there are interventions that alter IFNγ responsiveness in lung MNP subsets to affect infection outcome. Elucidating cell-specific actions of IFNγ is crucial for a comprehensive understanding of IFNγ-mediated immunity in tuberculosis, to make it more effective.

In this study, we identify subset-specific differences in IFNγ responsiveness across distinct lung MNP subsets during Mtb infection. Specifically, compared with AM, Mtb-permissive MNC1 cells are less responsive to IFNγ and exhibit defective IFNγ signal transduction, while MNC2 cells exhibit intermediate responsiveness to IFNγ. Compared with AM and MNC2 cells, MNC1 cells express less MHC-II and have a reduced ability to present Mtb antigens to CD4 T cells, which is partially dependent on Type I IFN signaling. We further found that prior Mtb immunity can improve IFNγ responsiveness of MNC cells, leading to better Mtb control. Together, these findings provide mechanistic insights into the functional heterogeneity of lung MNP subsets during TB, suggesting

that targeting IFNγ responsiveness may represent a strategy for developing novel TB therapies and vaccines.

Results

Differential responses to IFNγ in MNP subsets from *M. tuberculosis*-infected lungs.

To investigate if lung MNP subsets might respond to IFNγ differently during chronic Mtb infection, we first analyzed our bulk RNA-seq data for three flow-sorted lung MNP subsets (AM, CD11c^{lo} MNC1, and CD11c^{hi} MNC2) from mice infected with Mtb for 28 days (GSE220147) (Figure S1)[8]. Gene Ontology (GO) analysis revealed that IFNγ-responsive genes were expressed at significantly lower levels in MNC1 compared to AM or MNC2 (Table S1). We further investigated the expression levels of IFNγ-responsive genes in a published gene list[6,18]. In this analysis, MNC1 cells exhibited decreased expression of IFNγ-responsive genes compared to AM and MNC2 (Figure 1A), suggesting that this lung cell subset responds to IFNγ less effectively. Since IFNγ receptors and downstream regulators/proteins in the pathway dictate the cellular response to IFNγ (Figure 1B), we investigated their expression levels. This revealed that MNC1 had lower mRNA expression of *Ifngr1, Ifngr2*, *Stat1*, *Irf1*, *Cxcl9*, and *Nos2* compared to MNC2, while AM expressed significantly more *Ifngr2* mRNA than MNC1, with a similar but non-significant trend observed for *Ifngr1, Stat1*, and *Cxcl9* (Figure 1C). Using flow cytometry, we confirmed that MNC1 expressed lower levels of IFNGR2, STAT1, and IRF1 proteins, as well as the IFNγ-responsive proteins CXCL9 and NOS2, compared to AM or MNC2 (Figure 1D and Figure S2). Although AM expressed more IFNGR1 protein than MNC1, the protein level of IFNGR1 did not differ between MNC1 and MNC2 (Figure 1D and Figure S2). Together, these findings indicate that there are differential signaling and responses to IFNγ in these lung MNP subsets.

MNC1 are deficient in responding to IFNγ ex vivo.

Based on the above findings, we hypothesized that lung MNP subsets isolated from lungs during chronic Mtb infection either differ in their ability to respond to IFNγ, or that differential responses were due to differential exposure to IFNγ, perhaps due to their positioning or access to IFNγ in vivo. To distinguish these two possibilities, we compared responses to ex vivo IFNγ stimulation for lung MNP subsets by flow cytometric analysis of tyrosine phosphorylated STAT1 (pSTAT1), a key early signaling step in IFNγ cell activation. We prepared lung single-cell suspensions from Mtb-infected mice (28 dpi) and treated them with or without IFNγ (Figure 2A). Without IFNγ stimulation, AM and MNC2 showed higher pSTAT1 levels than MNC1, likely reflecting IFNγ stimulation in vivo. With ex vivo IFNγ stimulation, AM, MNC1, and MNC2 exhibited a 5.1-fold, 2.3-fold, and 2.5-fold increase of pSTAT1, respectively (Figure 2B-2C and Figure S2); however, MNC1 still showed a lower pSTAT1 signal than AM or MNC2 (Figure 2B). Interestingly, although infected AM and infected MNC2 responded to IFNγ better than their bystander counterparts, the subset difference in IFNγ responsiveness between AM, MNC1, and MNC2 did not depend on the presence of Mtb in individual cells (Figure S3). We also observed a similar phenotype at later time points of Mtb infection (Figure S4).

Since pSTAT1 functions in the nucleus, we used immunofluorescence to quantify nuclear pSTAT1 in sorted mononuclear cells with or without ex vivo IFNγ. In the absence of added IFNγ, the nuclear pSTAT1 level was similar in cells in all three subsets (Figure 2D). However, after IFNγ stimulation, we observed that MNC1 cells exhibited lower nuclear pSTAT1 levels than AM and MNC2, while MNC2 had an intermediate level between those of AM and MNC1 (Figure 2E). Furthermore, in response to IFNγ stimulation, MNC1 showed a lower fold change of nuclear pSTAT1 (1.5-fold) than AM (4.3-fold) or MNC2 (2.4-fold) (Figure 2F). Collectively, these results indicate that responsiveness to IFNγ is impaired at a proximal step of signal transduction in MNC1 compared with AM or MNC2, while MNC2 has an intermediate level of IFNγ responsiveness.

MNC1 are impaired for activating Mtb antigen-specific CD4 T cells.

One effect of IFNγ is to upregulate MHC-II, which mediates antigen presentation and CD4 T cell activation[19–21]. Therefore, we hypothesized that MNP subsets that differ in IFNγ responsiveness also differ in MHC-II expression and antigen presentation. GO analysis revealed that transcripts encoding multiple components of the MHC-II antigen presentation pathway are differentially regulated when comparing AM or MNC2 to MNC1 (Table S2). We found that class II transactivator (CIITA), the master transcription factor for MHC-II expression and other MHC-II antigen presentation-related genes is underexpressed in MNC1 (Figure 3A). Using flow cytometry, we confirmed that MHC-II and CD74 (the MHC-II invariant chain) are expressed at lower levels in MNC1 cells compared to AM and MNC2 (Figure 3B-3C and Figure S2). Differential MHC-II expression was also observed at 42 dpi and 56 dpi (Figure S5). Next, we sought to determine whether reduced MNC1 expression of MHC-II impairs antigen presentation to CD4 T cells. To specifically study antigen presentation independently of potential differences in antigen processing, we incubated sorted cells from MNP subsets from Mtb-infected mice with C7 or P25 epitope peptides (from ESAT-6 or Ag85B, respectively), and antigen-specific Th1-polarized C7 or P25 TCR transgenic CD4 T cells, then used IFNγ ELISA as a readout of T cell activation (Figure 3D). Consistent with the levels of expression of MHC-II pathway molecules, we observed lower responses by antigen-specific CD4 T cells when stimulated by MNC1 compared with AM or MNC2 (Figure 3E-3F), confirming that MNC1 cells have an impaired ability to present Mtb antigens to CD4 T cells.

Type I IFN inhibits MHC-II expression in primary macrophages and lung MNPs

We next investigated the potential mechanisms regulating MHC-II expression in lung MNP subsets. From our bulk RNA-seq data, we found a higher type I IFN signature in MNC1 and MNC2 compared to AM (Figure 4A), consistent with results from our prior study[4]. Since type I IFN has been reported to cause down-regulation of IFNGR [22–24], we reasoned that type I IFN might suppress IFNγ-mediated MHC-II upregulation in MNPs/macrophages in Mtb infection. To test this, we differentiated bone marrow-derived macrophages (BMDM) in the presence of IFNγ and/or IFNβ, and quantified MHC-II expression by flow cytometry. As expected, IFNγ significantly increased MHC-II in wild-type (WT) BMDM (Figure 4B). IFN-β alone slightly reduced MHC-II expression and inhibited IFNγ-mediated MHC-II upregulation. Deletion of the type I IFN receptor, *Ifnar1*, completely negated the inhibitory effect of IFNβ on MHC-II expression in BMDM (Figure 4C).

161 To further investigate the effect of type I IFN on MHC-II expression on different MNP subsets in
162 vivo, we generated mixed bone marrow chimeric mice (Figure 4D). Irradiated WT recipient mice
163 received WT and *Ifnar1*$^{-/-}$ mixed bone marrow cells. After reconstitution, the mice were infected
164 with Mtb by aerosol and harvested 28 dpi. All *Ifnar1*$^{-/-}$ lung MNP subsets showed higher MHC-II
165 expression compared to the analogous WT subsets (Figure 4E and Figure S6). Together, these
166 results indicate that type I IFN negatively regulates IFNγ-mediated MHC-II expression in BMDM
167 in vitro and in lung MNP subsets in vivo in the context of Mtb infection.

168

169 **CoMtb-mediated prior immunity improves IFNγ responsiveness of MNC cells but not AM**

170 Since monocytes and macrophages are functionally reprogrammable, we investigated whether
171 pre-existing immunity alters IFNγ responsiveness of MNP subsets, using the contained Mtb
172 (CoMtb) model[25]. This model is established by intradermal infection of Mtb in the mouse ear,
173 which results in Mtb trafficking to the local draining lymph nodes without bacterial dissemination
174 to other organs, including the lungs.

175 Since MNC cells are derived from monocytes[4,8,26,27], we first asked whether CoMtb regulates IFNγ
176 responsiveness in bone marrow monocytes ex vivo. For this, we established CoMtb for 4-6 weeks
177 (Figure 5A), then harvested bone marrow cells from CoMtb and control mice. Without IFNγ
178 stimulation, we observed higher pSTAT1 in CoMtb bone marrow monocytes compared with
179 control monocytes (Figure 5B). After IFNγ stimulation, CoMtb monocytes showed greater STAT1
180 activation than control monocytes; BMDM cultured from CoMtb mice also exhibited greater
181 pSTAT1 than did BMDM from control mice. These data suggest that CoMtb conditions monocytes
182 and macrophages to improve their IFNγ responsiveness in vivo (Figure 5B-5C).

183 We further investigated the effect of CoMtb on IFNγ responsiveness in lung MNP subsets from
184 mice after subsequent aerosol Mtb infection. Using flow cytometry detection of pSTAT1 to
185 quantitate IFNγ responses, we found that CoMtb improved responses to IFNγ in MNC1 and MNC2
186 cells, but not in AM, (Figure 5D). CoMtb also increased expression of IFNGR2 and the IFNγ-
187 regulated proteins MHC-II and NOS2 (Figure 5B). These results indicate that CoMtb improves
188 IFNγ responsiveness in monocyte-derived cells that traffic to the lungs after aerosol Mtb challenge.

189

190 **CoMtb-mediated control of Mtb in lung monocyte-derived cells requires IFNγ signaling**

191 As indicated by whole lung CFU, we confirmed that CoMtb reduced Mtb burden in the lung after
192 aerosol infection (Figure 6A); we also found that CoMtb reduced the number of total Mtb-infected
193 cells in the lungs and lower bacterial fluorescence intensity (indicative of the per-cell bacterial
194 burden) in the infected cells (Figure 6B-6C). We further found that CoMtb decreased the number
195 of infected AM, MNC1, MNC2, and neutrophils compared to controls (Figure 6D). In addition, the
196 infection frequency (i.e., the percentage of cells in a given subset that contain Mtb) was reduced
197 in all subsets when comparing CoMtb mice to control mice (Figure 6E). Moreover, we found that
198 CoMtb reduced Mtb burdens in AM (1.2-fold decrease), neutrophils (1.5-fold decrease), and
199 especially in MNC1 (2.7-fold decrease) and MNC2 (1.8-fold decrease) (Figure 6F). In line with
200 these results, chimeric mice that received bone marrow from CoMtb mice showed lower lung CFU
201 burdens than mice that received control bone marrow cells (Figure 6G-6H). Thus, these findings

202 indicate that improved IFNγ responsiveness can enhance Mtb control in monocyte-derived lung
203 cells.

204 We next sought to determine whether IFNγ responsiveness is required for CoMtb-mediated Mtb
205 control in MNC cells. For this, we generated mixed bone marrow chimeric mice (Figure 6I).
206 Irradiated WT mice received WT and *Ifngr1*$^{-/-}$ mixed bone marrow cells (1:1). After reconstitution
207 and CoMtb establishment, they were infected with Mtb by aerosol and harvested at 28 dpi. This
208 revealed higher bacterial burdens in *Ifngr1*$^{-/-}$ myeloid cells compared to WT myeloid cells from the
209 same chimeric mouse (Figure 6J and Figure S7). Similarly, we observed a higher Mtb burden in
210 *Ifngr1*$^{-/-}$ MNC cells compared to WT counterparts (Figure 6J-6K). However, we observe a slight
211 difference in Mtb burden between WT and *Ifngr1*$^{-/-}$ AM at 28 dpi (Figure 6J), consistent with our
212 data showing that CoMtb plays a minimal role in AM at the later stage of Mtb infection, in contrast
213 to the effect of CoMtb on AM at an early stage of infection[25]. Collectively, these results suggest
214 that CoMtb-mediated prior immunity enhances Mtb control in MNC cells, which depends on IFNγ
215 signaling.

216

217 **Discussion**

218 A predominant adaptive immune response to Mtb infection in mice, nonhuman primates, and
219 humans is represented by T lymphocytes that produce IFNγ[15,19,28–34], a cytokine that plays an
220 essential role in activating macrophages to restrict diverse intracellular pathogens. We and others
221 have determined that Mtb resides in multiple macrophage subsets in the lungs[4,7–10,20,35–38].
222 However, immunity to TB is often incomplete despite abundant IFNγ production, and increasing
223 IFNγ levels alone does not necessarily improve bacterial control in the lungs [1 17] . Together, these
224 results suggest that while IFNγ is necessary, its efficacy may be limited by impaired cellular
225 responses and other inhibitory mechanisms in vivo that blunt the effects of IFNγ. This paradox
226 highlights the need to better understand the mechanisms regulating IFNγ responsiveness in lung
227 macrophage subsets to develop more effective TB therapies and vaccines.

228 Here, we identified a previously undefined mechanism that contributes to the suboptimal efficacy
229 of IFNγ in immunity to Mtb. Using an unbiased initial approach, bulk RNA sequencing of flow-
230 sorted mononuclear-macrophage cell subsets (AM and two subsets of lung monocyte-derived
231 cells), we detected evidence that one of the monocyte-derived cell subsets (termed MNC1,
232 formerly termed recruited macrophages) expresses lower levels of transcripts for IFNγ-responsive
233 genes when compared with AM or the other monocyte-derived cell subset (MNC2). Since this
234 could have reflected differential exposure of these cells to IFNγ in vivo, we treated lung cell
235 suspensions ex vivo with IFNγ and found that MNC1 cells are less responsive to IFNγ as
236 manifested by reduced tyrosine phosphorylation of STAT1. We also found that at the levels of
237 mRNA and cell surface expression, MNC1 cells express lower levels of the IFNγ receptor subunit,
238 IFNGR2, and other key signaling molecules in the response to IFNγ, including STAT1 and IRF1.
239 These results indicate that in MNC1 cells, defective responses to IFNγ are associated with
240 reduced expression of the proximal signaling machinery required for cell responses to IFNγ, and
241 this results in reduced responses to IFNγ in these cells. Our findings complement in vitro
242 observations that cultured macrophages infected with Mtb are defective in responding to IFNγ
243 through multiple mechanisms. These mechanisms include prolonged TLR2 signaling initiated by

Mtb lipoproteins and other cell wall components[39–44], and inhibition of macrophage responses to IFNγ by IL-6 [45]. Notably, these mechanisms inhibit IFNγ-responsive gene expression at one or more steps downstream of STAT1 activation and function[46,47]. Although the in vivo relevance of these mechanisms inhibiting macrophage responses to IFNγ has not been established, our study highlights a distinct, subset-specific pathway of IFNγ signaling impairment in MNC1 cells during chronic Mtb infection (Figure 7).

Recent studies reveal that the Mtb-killing ability in distinct macrophage subsets differs with the stage of infection. In early infection prior to development of adaptive T cell responses, AM are permissive to Mtb[35–37], while after adaptive T lymphocytes are primed and recruited to the lungs, AM restrict Mtb more effectively than do monocyte-derived cells [4,7–10]. Specifically, we previously reported that MNC1 cells harbor more viable Mtb per infected cell than do AM and MNC2 cells during chronic infection[8]. Adaptive T cells contribute to determining the fate and state of Mtb in distinct lung mononuclear cell subsets, and T cells have a greater impact on suppressing Mtb in AM than in recruited mononuclear cells in the lungs[7]. Our work extends these findings by demonstrating that subset-specific differences in IFNγ responsiveness may explain why T cell-mediated adaptive immunity has a greater impact on bacterial control in AM than in monocyte-derived cells, indicating that impaired IFNγ responsiveness contributes to Mtb permissiveness.

Although we have not yet fully identified the regulatory pathway(s) responsible for reduced expression of the signaling molecules required for responses to IFNγ, we found that type I IFN signaling contributes to reduced IFNγ-mediated MHC-II expression in MNC1 cells, impairing their ability to present antigens to antigen-specific CD4+ T cells. This provides a mechanistic link between the known detrimental role of Type I IFN in TB and the failure of $CD4^+$ T-cell-mediated control at the cellular level. Although MNC2 cells express higher mRNA levels of IFNγ pathway genes, they are less responsive to IFNγ stimulation compared to AM. This suggests that MNC2 may be exposed to higher levels of IFNγ than AM cells, likely due to their localization. However, MNC2 show a greater type I IFN signaling than AM, which may antagonize IFNγ signaling. Interestingly, IFNγ responsiveness in MNC1 is not fully restored by deletion of *Ifnar1*, suggesting that other mechanisms may contribute to regulating IFNγ responsiveness in lung MNC subsets in vivo during Mtb infection.

An important discovery from this study is that the impaired IFNγ responsiveness of MNC1 cells is not an irreversible differentiation trait but rather a malleable phenotype that can be reprogrammed by prior immunity (Figure 7). We found that the responsiveness of MNC1 cells to IFNγ can be modulated: pre-existing immunity established by CoMtb modifies bone marrow precursors of MNC1 and MNC2 cells to improve their responses to IFNγ and improve their ability to control Mtb. In this manner, our results are consistent with trained immunity[48], since we found that the impact of CoMtb on myeloid cells influenced ex vivo responses to IFNγ and that transfer of bone marrow cells from mice with CoMtb improved control of Mtb after aerosol challenge. While deleting the IFNγ receptor slightly increased bacterial burden in AM from coMtb mice, the impact of IFNγR deletion on bacterial control is more pronounced in monocyte-derived cells. This aligns with a recent study showing that CoMtb induces IFNγ signaling in MNC cells from Mtb-susceptible mice[49]. These findings indicate that the mechanisms of enhanced immunity in CoMtb mice are cell-type specific. MNC1 cells face a critical 'bottleneck' due to impaired IFNγ signaling during primary infection; thus, restoring this responsiveness via CoMtb is a primary driver of their

287 improved control. In contrast, while IFNγR signaling contributes to AM function at early
288 stages[25,50,51], it plays a more limited role in the CoMtb-mediated protection of AMs during the later
289 chronic stage of infection. However, we cannot exclude the possibility that CoMtb may alter other
290 cell-intrinsic mechanisms, such as lysosome biogenesis and autophagy, to synergize with
291 improved IFNγ responsiveness and enhance bacterial control, which warrants further study.
292 Together, these results indicate that modulation of MNC1 cells can be achieved, suggesting that
293 this may be an especially valuable target for host-directed TB therapies.

294 We also note that the cell subset (MNC1) that is deficient in responses to IFNγ is the same subset
295 that we previously reported as being deficient in lysosome biogenesis. Since there are no known
296 regulatory connections between IFNγ responsiveness and lysosome biogenesis, our results are
297 most consistent with a model in which both pathways are regulated by a common developmental
298 pathway during differentiation of bone marrow monocytes into monocyte-derived macrophages in
299 the lungs of Mtb-infected mice. Further investigation of the differentiation or maturation of
300 monocytes recruited to the lungs in response to Mtb will be needed for a more thorough
301 understanding of the determinants of cell responsiveness to IFNγ and of lysosome biogenesis.

302 A shortcoming of the studies reported here is that they only involved studies in mice. Recent
303 single-cell sequencing studies have revealed heterogeneity of lung monocyte-derived
304 macrophages in human TB[52–54], and a potential difference in IFNγ responses among macrophage
305 subsets in TB granulomas[52]. However, functional studies are required to characterize IFNγ
306 responsiveness in live macrophage subsets isolated from resected lung tissues of human TB
307 patients. These are limited by the rarity of appropriate human samples in proximity to facilities for
308 the procedures required, and considerable dedicated effort will be required to determine which of
309 our findings are applicable to humans. Nevertheless, our results provide further mechanistic
310 insight into the potential functional significance of macrophage heterogeneity in the lungs in the
311 context of Mtb infection and should drive further investigation of methods to optimally develop and
312 test host-directed therapies for TB.

313

314

315 **Methods**

316 **Mice**

317 8-12-week-old C57BL/6 (Strain #:000664), *Ifnar1*$^{-/-}$ (Strain #:028288) and *Ifngr1*$^{-/-}$ (Strain
318 #:003288) mice were obtained from Jackson Laboratory. Both sexes were used in this study.
319 Extensive experiments and projects in our lab demonstrate no sex-specific differences in our
320 murine TB models. Therefore, sex was not a consideration in this study; sample sex information
321 has not been collected. Mice infected with Mtb were housed in the Animal Biosafety Level 3
322 facility. All animal experiments were approved by the Institutional Animal Care and Use
323 Committee of the University of California, San Francisco.

324 **Bacterial strains, growth, and aerosol infection**

325 Mtb H37Rv was transformed with pMV261::ZsGreen and cultured in Middlebrook 7H9 medium
326 (BD) supplemented with 10% (v/v) ADC (albumin, dextrose, catalase), 0.05 % Tween 80, 0.2 %
327 glycerol, and 50 µg/ml kanamycin[8]. Mice were infected with H37Rv or pMV261::ZsGreen via
328 aerosol using a Glas-Col inhalation exposure unit, as previously described[4,8,26,38]. Mid-log cultures

329 were centrifuged at 800g for 8 min. Clump-free cultures were transferred and diluted, and 5 mL
330 of inoculum was added to the nebulizer. The target dose was 100 CFU/mouse. Infection dose
331 was determined by plating lung homogenates 24 hours post-infection on 7H11 agar plates. CFUs
332 were counted after incubation of plates at 37°C for 3 weeks.

333 **Lung homogenate preparation, flow cytometry, and cell sorting**

334 Lung homogenates were prepared as described previously[4,8]. Lungs were perfused with 10 mL
335 of PBS/2 mM EDTA via the right ventricle immediately after euthanasia. Lungs were processed
336 with a gentleMACS dissociator (Miltenyi, lung program 1), and digested in 4 mL of RPMI-1640/5%
337 HI-FBS containing 1 mg/mL collagenase D (Sigma-Aldrich) and 50 µg/mL DNase I (Sigma-
338 Aldrich) for 30 min at 37 °C. Digested lung tissues were further dissociated with the gentleMACS
339 dissociator (lung program 2) and then passed through a 70-µm cell strainer. Red blood cells were
340 lysed with 3 mL ACK lysis buffer (Gibco) for 3 min and washed twice with RPMI-1640/5% HI-FBS.
341
342 For staining of surface antigens, cells were washed with PBS, then stained with 1:200 Zombie
343 Aqua Fixable Viability Dye (BioLegend, 423101) and 1:100 anti-CD16/32 (clone 2.4G2; Fc
344 receptor blockade) for 15 min at 4°C. After washing with PBS, cells were stained with flow
345 antibodies from Table S3 in 1:1 PBS/Brilliant Stain Buffer (BD, 566349) for 30 min at 4°C. Samples
346 were washed twice with PBS, then fixed overnight in 1% paraformaldehyde (PFA)/PBS. For cell
347 sorting, cells were washed and resuspended in FACS buffer (PBS, 2% HI-FBS (v/v), 2 mM EDTA
348), and sorting was done using the BSL3 Sony MAC900 cell sorter.

349 For intracellular staining, cells were fixed and permeabilized using BD Fixation/Permeabilization
350 Kit for 20 min at 4°C after surface staining, then washed and incubated with antibodies diluted in
351 1x BD Perm Wash/0.5% FBS for 30 min at RT. For IRF1, 0.1% Triton X-100/PBS was used for
352 permeabilization. Samples were washed and acquired using an Aurora spectral flow cytometer
353 (Cytek Biosciences) or Sony MA900.

354 **Ex vivo IFNγ stimulation for pSTAT1 flow cytometry**

355 10^6 cells per lung were stained with Zombie Aqua Fixable Viability Dye as described above at 4°C
356 for 15 min. Samples were washed once with RPMI-1640/5% HI-FBS, then stimulated with 100 µL
357 of 20ng/mL IFNγ (final concentration) (Biolegend, 575304) in media at 37°C for 15 min. Untreated
358 samples were kept at 4°C. Samples were then mixed with 100 µL of 4% PFA/PBS and fixed at
359 room temperature (RT) for 15 min. Cells were washed once with PBS, followed by
360 permeabilization with 180 µL of cold methanol at 4°C for 12 min. After this, samples were washed
361 twice and incubated with 50 µL of 1:50 anti-CD16/32 in PBS for 5 min, followed by the addition of
362 antibodies, including AF647-pSTAT1 (Cell Signaling Technology, 8009S), diluted in 50 µL of
363 Brilliant Stain Buffer and incubated for 30 min at RT. After washing twice with PBS, samples were
364 resuspended in 1% PFA/PBS.

365 **Immunofluorescence**

366 Lung cell subsets were sorted from mice infected with H37Rv-ZsGreen. 40,000 cells/well were
367 seeded into 8-well Nunc Lab-Tek chamber slides (Thermo Scientific, 177445), and rested in a cell
368 incubator for 1 h. Media were replaced with 100 µL of RPMI-1640/5% HI-FBS with or without
369 20ng/mL IFNγ, and cells were incubated for 15min at 37°C. Immunofluorescence was performed
370 as previously described with slight modifications[8,55,56]. Media were removed and cells were fixed

371 immediately with 4% PFA for 30min. Slides were immersed in 1% PFA/PBS and transferred to
372 BSL2. Cells were washed twice with 200 µL PBS, followed by permeabilization with 200 µL of ice-
373 cold methanol for 10 min at 4°C, and then washed 3 times with PBS. Samples were blocked with
374 5% goat serum/PBS for 30 min at RT, then incubated with 100 µL of pStat1 (Tyr701) Rabbit mAb
375 (Cell Signaling Technology, 9167S, 1:200 diluted in 5% goat serum/PBS) for 2 h at RT. Then cells
376 were washed three times with PBS and stained with 1:1000 Goat anti-Rabbit IgG AF647
377 (Invitrogen, A-21244) for 1 h at RT. Samples were washed three times with PBS and mounted
378 with ProLong Diamond Antifade Mountant with DAPI.

379 **T cell and MNP coculture**

380 T cell and MNP coculture were done as described previously[21,57]. ZsGreen^{-} Lung MNP subsets
381 (AM, MNC1 and MNC2) were sorted from mice infected with H37Rv-ZsGreen. 10,000/well of MNP
382 were cultured with P25TCR-Tg or C7TCR-Tg Th1 effector cells (200,000/well) in the presence of
383 10 µg/mL Ag85B peptide 25. Supernatants were collected at day 4 and assayed for IFNγ by
384 ELISA.

385

386 **BMDM differentiation**

387 BMDM were differentiated as described previously[8]. Briefly, bone marrow cells were cultured in
388 BMDM media [DMEM (Gibco, 11965092), 10% heat-inactivated FBS (HI-FBS), and 20 ng/ml
389 recombinant murine M-CSF (PeproTech)] for 6-7 days, and media change was done at day 3.
390 For differentiation with interferon, BMDM media containing 50 pg/mL of IFNγ (Biolegend, 575304)
391 or IFN-β (Sino Biological, 50708-MCCH) were used. At day 6-7, cells were washed twice with
392 PBS and incubated with cold PBS/2mM EDTA for 5 min, then harvested by pipetting.

393

394 **Generation of bone marrow chimeras**

395 Bone marrow chimeras were generated as described previously[14]. Bone marrow cells were
396 harvested from the femurs and tibias of donor mice. After ACK lysis, cells were washed once with
397 DMEM/10% HI-FBS, once with PBS, then filtered with a 70 µm strainer. Recipient mice were
398 irradiated with a Precision X-Rad320 X-Ray irradiator using a dose of 10 Gy. Within 24h post-
399 irradiation, 6×10^{6} total bone marrow cells were retro-orbitally injected into recipient mice using a
400 28G insulin syringe. For the chimera experiment using bone marrow cells from control or CoMtb
401 mice, recipient mice received $5\text{x}10^{6}$ T cell-depleted bone marrow cells. Irradiated mice were
402 given TMP-SMX antibiotic (Sulfamethoxazole and Trimethoprim Oral Suspension, 200 mg/40 mg
403 per 5 mL, use 7.5 mL per 293 mL drinking water) for 3 weeks. Mice were allowed to reconstitute
404 for at least 6-8 weeks.

405 **Establishment of CoMtb**

406 CoMtb was established as described previously[25]. Briefly, mice were anesthetized with isoflurane.
407 1×10^{4} CFU of Mtb H37Rv were injected intradermally into the base of the ear in 10 µL PBS using
408 a 31 G insulin syringe. After 4-6 weeks of establishment, mice were used for experiments.

409 **RNA sequencing and data analysis**

410 Analysis of the RNA-sequencing dataset GSE220147 was performed as described previously[8].

Quantification and statistical analysis

Results are expressed as mean and standard error. Quantification of MFI from immunofluorescence images was done using ImageJ, and the data are background-subtracted. MFI data for the lung subsets are background-subtracted using the fluorescence minus one (FMO) control or uninfected control. Statistical analysis and p-values are stated in the figure legends and indicated in the figures, respectively. $P < 0.05$ is considered significant.

Data availability

The RNA-seq data supporting the findings of this study are available in the Gene Expression Omnibus (GEO) under the accession number: GSE220147. Source data are provided with this paper.

References

1. Ernst, J.D. (2018). Mechanisms of M. tuberculosis Immune Evasion as Challenges to TB Vaccine Design. Cell Host Microbe *24*, 34–42. https://doi.org/10.1016/j.chom.2018.06.004.
2. Chandra, P., Grigsby, S.J., and Philips, J.A. (2022). Immune evasion and provocation by Mycobacterium tuberculosis. Nat Rev Microbiol *20*, 750–766. https://doi.org/10.1038/s41579-022-00763-4.
3. Lefrançais, E., Hudrisier, D., Neyrolles, O., Behar, S.M., and Ernst, J.D. (2025). Finding and filling the knowledge gaps in mechanisms of T cell-mediated TB immunity to inform vaccine design. Nat Rev Immunol. https://doi.org/10.1038/s41577-025-01192-z.
4. Zheng, W., Borja, M., Dorman, L.C., Liu, J., Zhou, A., Seng, A., Arjyal, R., Sunshine, S., Nalyvayko, A., Pisco, A.O., et al. (2025). Single-cell analysis reveals Mycobacterium tuberculosis ESX-1-mediated accumulation of permissive macrophages in infected mouse lungs. Sci Adv *11*, eadq8158. https://doi.org/10.1126/sciadv.adq8158.
5. Pisu, D., Huang, L., Narang, V., Theriault, M., Lê-Bury, G., Lee, B., Lakudzala, A.E., Mzinza, D.T., Mhango, D.V., Mitini-Nkhoma, S.C., et al. (2021). Single cell analysis of M. tuberculosis phenotype and macrophage lineages in the infected lung. J Exp Med *218*, e20210615. https://doi.org/10.1084/jem.20210615.

6. Kotov, D.I., Lee, O.V., Fattinger, S.A., Langner, C.A., Guillen, J.V., Peters, J.M., Moon, A., Burd, E.M., Witt, K.C., Stetson, D.B., et al. (2023). Early cellular mechanisms of type I interferon-driven susceptibility to tuberculosis. Cell *186*, 5536-5553.e22. https://doi.org/10.1016/j.cell.2023.11.002.

7. Lai, R., Williams, T., Rakib, T., Lee, J., and Behar, S.M. (2024). Heterogeneity in lung macrophage control of Mycobacterium tuberculosis is modulated by T cells. Nat Commun *15*, 5710. https://doi.org/10.1038/s41467-024-48515-7.

8. Zheng, W., Chang, I.-C., Limberis, J., Budzik, J.M., Zha, B.S., Howard, Z., Chen, L., and Ernst, J.D. (2024). Mycobacterium tuberculosis resides in lysosome-poor monocyte-derived lung cells during chronic infection. PLoS Pathog *20*, e1012205. https://doi.org/10.1371/journal.ppat.1012205.

9. Lee, J., Boyce, S., Powers, J., Baer, C., Sassetti, C.M., and Behar, S.M. (2020). CD11cHi monocyte-derived macrophages are a major cellular compartment infected by Mycobacterium tuberculosis. PLoS Pathog *16*, e1008621. https://doi.org/10.1371/journal.ppat.1008621.

10. Wolf, A.J., Linas, B., Trevejo-Nuñez, G.J., Kincaid, E., Tamura, T., Takatsu, K., and Ernst, J.D. (2007). Mycobacterium tuberculosis infects dendritic cells with high frequency and impairs their function in vivo. J Immunol *179*, 2509–2519. https://doi.org/10.4049/jimmunol.179.4.2509.

11. Casanova, J.-L., MacMicking, J.D., and Nathan, C.F. (2024). Interferon-γ and infectious diseases: Lessons and prospects. Science *384*, eadl2016. https://doi.org/10.1126/science.adl2016.

12. Flynn, J.L., Chan, J., Triebold, K.J., Dalton, D.K., Stewart, T.A., and Bloom, B.R. (1993). An essential role for interferon gamma in resistance to Mycobacterium tuberculosis infection. J Exp Med *178*, 2249–2254. https://doi.org/10.1084/jem.178.6.2249.

13. Cooper, A.M., Dalton, D.K., Stewart, T.A., Griffin, J.P., Russell, D.G., and Orme, I.M. (1993). Disseminated tuberculosis in interferon gamma gene-disrupted mice. J Exp Med *178*, 2243–2247. https://doi.org/10.1084/jem.178.6.2243.

14. Desvignes, L., and Ernst, J.D. (2009). Interferon-gamma-responsive nonhematopoietic cells regulate the immune response to Mycobacterium tuberculosis. Immunity *31*, 974–985. https://doi.org/10.1016/j.immuni.2009.10.007.

15. Maciag, K., Plumlee, C.R., Cohen, S.B., Gern, B.H., and Urdahl, K.B. (2024). Reappraising the Role of T Cell-Derived IFN-γ in Restriction of Mycobacterium tuberculosis in the Murine Lung. J Immunol *213*, 339–346. https://doi.org/10.4049/jimmunol.2400145.

16. Bustamante, J., Boisson-Dupuis, S., Abel, L., and Casanova, J.-L. (2014). Mendelian susceptibility to mycobacterial disease: genetic, immunological, and clinical features of inborn errors of IFN-γ immunity. Semin Immunol *26*, 454–470. https://doi.org/10.1016/j.smim.2014.09.008.

17. Sakai, S., Kauffman, K.D., Sallin, M.A., Sharpe, A.H., Young, H.A., Ganusov, V.V., and Barber, D.L. (2016). CD4 T Cell-Derived IFN-γ Plays a Minimal Role in Control of Pulmonary Mycobacterium tuberculosis Infection and Must Be Actively Repressed by PD-1 to Prevent Lethal Disease. PLoS Pathog *12*, e1005667. https://doi.org/10.1371/journal.ppat.1005667.

18. Melo-Silva, C.R., Roman, M.I., Knudson, C.J., Tang, L., Xu, R.-H., Tassetto, M., Dolan, P., Andino, R., and Sigal, L.J. (2022). Interferon partly dictates a divergent transcriptional response in poxvirus-infected and bystander inflammatory monocytes. Cell Rep *41*, 111676. https://doi.org/10.1016/j.celrep.2022.111676.

493 19. Mogues, T., Goodrich, M.E., Ryan, L., LaCourse, R., and North, R.J. (2001). The relative
494 importance of T cell subsets in immunity and immunopathology of airborne Mycobacterium
495 tuberculosis infection in mice. J Exp Med *193*, 271–280.
496 https://doi.org/10.1084/jem.193.3.271.

497 20. Srivastava, S., and Ernst, J.D. (2013). Cutting edge: Direct recognition of infected cells by
498 CD4 T cells is required for control of intracellular Mycobacterium tuberculosis in vivo. J
499 Immunol *191*, 1016–1020. https://doi.org/10.4049/jimmunol.1301236.

500 21. Srivastava, S., and Ernst, J.D. (2014). Cell-to-cell transfer of M. tuberculosis antigens
501 optimizes CD4 T cell priming. Cell Host Microbe *15*, 741–752.
502 https://doi.org/10.1016/j.chom.2014.05.007.

503 22. Eshleman, E.M., Delgado, C., Kearney, S.J., Friedman, R.S., and Lenz, L.L. (2017). Down
504 regulation of macrophage IFNGR1 exacerbates systemic L. monocytogenes infection. PLoS
505 Pathog *13*, e1006388. https://doi.org/10.1371/journal.ppat.1006388.

506 23. Kearney, S.J., Delgado, C., Eshleman, E.M., Hill, K.K., O'Connor, B.P., and Lenz, L.L. (2013).
507 Type I IFNs downregulate myeloid cell IFN-γ receptor by inducing recruitment of an early
508 growth response 3/NGFI-A binding protein 1 complex that silences ifngr1 transcription. J
509 Immunol *191*, 3384–3392. https://doi.org/10.4049/jimmunol.1203510.

510 24. Rayamajhi, M., Humann, J., Penheiter, K., Andreasen, K., and Lenz, L.L. (2010). Induction of
511 IFN-alphabeta enables Listeria monocytogenes to suppress macrophage activation by IFN-
512 gamma. J Exp Med *207*, 327–337. https://doi.org/10.1084/jem.20091746.

513 25. Nemeth, J., Olson, G.S., Rothchild, A.C., Jahn, A.N., Mai, D., Duffy, F.J., Delahaye, J.L.,
514 Srivatsan, S., Plumlee, C.R., Urdahl, K.B., et al. (2020). Contained Mycobacterium
515 tuberculosis infection induces concomitant and heterologous protection. PLoS Pathog *16*,
516 e1008655. https://doi.org/10.1371/journal.ppat.1008655.

517 26. Mohapatra, A., Norris, B.A., Howard, Z., and Ernst, J.D. (2025). CCR2 recruits monocytes to
518 the lung, while CX3CR1 modulates positioning of CD11cpos cells in the lymph node during
519 pulmonary tuberculosis. mBio, e0123725. https://doi.org/10.1128/mbio.01237-25.

520 27. Norris, B.A., and Ernst, J.D. (2018). Mononuclear cell dynamics in M. tuberculosis infection
521 provide opportunities for therapeutic intervention. PLoS Pathog *14*, e1007154.
522 https://doi.org/10.1371/journal.ppat.1007154.

523 28. Green, A.M., Difazio, R., and Flynn, J.L. (2013). IFN-γ from CD4 T cells is essential for host
524 survival and enhances CD8 T cell function during Mycobacterium tuberculosis infection. J
525 Immunol *190*, 270–277. https://doi.org/10.4049/jimmunol.1200061.

526 29. Leveton, C., Barnass, S., Champion, B., Lucas, S., De Souza, B., Nicol, M., Banerjee, D., and
527 Rook, G. (1989). T-cell-mediated protection of mice against virulent Mycobacterium
528 tuberculosis. Infect Immun *57*, 390–395. https://doi.org/10.1128/iai.57.2.390-395.1989.

529 30. Müller, I., Cobbold, S.P., Waldmann, H., and Kaufmann, S.H. (1987). Impaired resistance to
530 Mycobacterium tuberculosis infection after selective in vivo depletion of L3T4+ and Lyt-2+ T
531 cells. Infect Immun *55*, 2037–2041. https://doi.org/10.1128/iai.55.9.2037-2041.1987.

532 31. Lin, P.L., Rutledge, T., Green, A.M., Bigbee, M., Fuhrman, C., Klein, E., and Flynn, J.L. (2012).
533 CD4 T cell depletion exacerbates acute Mycobacterium tuberculosis while reactivation of
534 latent infection is dependent on severity of tissue depletion in cynomolgus macaques. AIDS
535 Res Hum Retroviruses *28*, 1693–1702. https://doi.org/10.1089/AID.2012.0028.

536 32. Yao, S., Huang, D., Chen, C.Y., Halliday, L., Wang, R.C., and Chen, Z.W. (2014). CD4+ T
537 cells contain early extrapulmonary tuberculosis (TB) dissemination and rapid TB progression

538 and sustain multieffector functions of CD8+ T and CD3- lymphocytes: mechanisms of CD4+
539 T cell immunity. J Immunol *192*, 2120–2132. https://doi.org/10.4049/jimmunol.1301373.

540 33. Kwan, C.K., and Ernst, J.D. (2011). HIV and tuberculosis: a deadly human syndemic. Clin
541 Microbiol Rev *24*, 351–376. https://doi.org/10.1128/CMR.00042-10.

542 34. Mayer-Barber, K.D., and Barber, D.L. (2015). Innate and Adaptive Cellular Immune
543 Responses to Mycobacterium tuberculosis Infection. Cold Spring Harb Perspect Med *5*,
544 a018424. https://doi.org/10.1101/cshperspect.a018424.

545 35. Huang, L., Nazarova, E.V., Tan, S., Liu, Y., and Russell, D.G. (2018). Growth of
546 Mycobacterium tuberculosis in vivo segregates with host macrophage metabolism and
547 ontogeny. J Exp Med *215*, 1135–1152. https://doi.org/10.1084/jem.20172020.

548 36. Cohen, S.B., Gern, B.H., Delahaye, J.L., Adams, K.N., Plumlee, C.R., Winkler, J.K., Sherman,
549 D.R., Gerner, M.Y., and Urdahl, K.B. (2018). Alveolar Macrophages Provide an Early
550 Mycobacterium tuberculosis Niche and Initiate Dissemination. Cell Host Microbe *24*, 439-
551 446.e4. https://doi.org/10.1016/j.chom.2018.08.001.

552 37. Rothchild, A.C., Olson, G.S., Nemeth, J., Amon, L.M., Mai, D., Gold, E.S., Diercks, A.H., and
553 Aderem, A. (2019). Alveolar macrophages generate a noncanonical NRF2-driven
554 transcriptional response to Mycobacterium tuberculosis in vivo. Sci Immunol *4*, eaaw6693.
555 https://doi.org/10.1126/sciimmunol.aaw6693.

556 38. Zha, B.S., Desvignes, L., Fergus, T.J., Cornelius, A., Cheng, T.-Y., Moody, D.B., and Ernst,
557 J.D. (2022). Bacterial Strain-Dependent Dissociation of Cell Recruitment and Cell-to-Cell
558 Spread in Early M. tuberculosis Infection. mBio *13*, e0133222.
559 https://doi.org/10.1128/mbio.01332-22.

560 39. Pai, R.K., Pennini, M.E., Tobian, A.A.R., Canaday, D.H., Boom, W.H., and Harding, C.V.
561 (2004). Prolonged toll-like receptor signaling by Mycobacterium tuberculosis and its 19-
562 kilodalton lipoprotein inhibits gamma interferon-induced regulation of selected genes in
563 macrophages. Infect Immun *72*, 6603–6614. https://doi.org/10.1128/IAI.72.11.6603-
564 6614.2004.

565 40. Gehring, A.J., Rojas, R.E., Canaday, D.H., Lakey, D.L., Harding, C.V., and Boom, W.H.
566 (2003). The Mycobacterium tuberculosis 19-kilodalton lipoprotein inhibits gamma interferon-
567 regulated HLA-DR and Fc gamma R1 on human macrophages through Toll-like receptor 2.
568 Infect Immun *71*, 4487–4497. https://doi.org/10.1128/IAI.71.8.4487-4497.2003.

569 41. Kincaid, E.Z., Wolf, A.J., Desvignes, L., Mahapatra, S., Crick, D.C., Brennan, P.J., Pavelka,
570 M.S., and Ernst, J.D. (2007). Codominance of TLR2-dependent and TLR2-independent
571 modulation of MHC class II in Mycobacterium tuberculosis infection in vivo. J Immunol *179*,
572 3187–3195. https://doi.org/10.4049/jimmunol.179.5.3187.

573 42. Fortune, S.M., Solache, A., Jaeger, A., Hill, P.J., Belisle, J.T., Bloom, B.R., Rubin, E.J., and
574 Ernst, J.D. (2004). Mycobacterium tuberculosis inhibits macrophage responses to IFN-
575 gamma through myeloid differentiation factor 88-dependent and -independent mechanisms.
576 J Immunol *172*, 6272–6280. https://doi.org/10.4049/jimmunol.172.10.6272.

577 43. Banaiee, N., Kincaid, E.Z., Buchwald, U., Jacobs, W.R., and Ernst, J.D. (2006). Potent
578 inhibition of macrophage responses to IFN-gamma by live virulent Mycobacterium
579 tuberculosis is independent of mature mycobacterial lipoproteins but dependent on TLR2. J
580 Immunol *176*, 3019–3027. https://doi.org/10.4049/jimmunol.176.5.3019.

581 44. Pai, R.K., Convery, M., Hamilton, T.A., Boom, W.H., and Harding, C.V. (2003). Inhibition of
582 IFN-gamma-induced class II transactivator expression by a 19-kDa lipoprotein from

583 Mycobacterium tuberculosis: a potential mechanism for immune evasion. J Immunol *171*,
584 175–184. https://doi.org/10.4049/jimmunol.171.1.175.

585 45. Nagabhushanam, V., Solache, A., Ting, L.-M., Escaron, C.J., Zhang, J.Y., and Ernst, J.D.
586 (2003). Innate inhibition of adaptive immunity: Mycobacterium tuberculosis-induced IL-6
587 inhibits macrophage responses to IFN-gamma. J Immunol *171*, 4750–4757.
588 https://doi.org/10.4049/jimmunol.171.9.4750.

589 46. Kincaid, E.Z., and Ernst, J.D. (2003). Mycobacterium tuberculosis exerts gene-selective
590 inhibition of transcriptional responses to IFN-gamma without inhibiting STAT1 function. J
591 Immunol *171*, 2042–2049. https://doi.org/10.4049/jimmunol.171.4.2042.

592 47. Ting, L.M., Kim, A.C., Cattamanchi, A., and Ernst, J.D. (1999). Mycobacterium tuberculosis
593 inhibits IFN-gamma transcriptional responses without inhibiting activation of STAT1. J
594 Immunol *163*, 3898–3906.

595 48. Khader, S.A., Divangahi, M., Hanekom, W., Hill, P.C., Maeurer, M., Makar, K.W., Mayer-
596 Barber, K.D., Mhlanga, M.M., Nemes, E., Schlesinger, L.S., et al. (2019). Targeting innate
597 immunity for tuberculosis vaccination. J Clin Invest *129*, 3482–3491.
598 https://doi.org/10.1172/JCI128877.

599 49. Gern, B.H., Klas, J.M., Foster, K.A., Kanagy, M.E., Cohen, S.B., Plumlee, C.R., Duffy, F.J.,
600 Neal, M.L., Halima, M., Gustin, A.T., et al. (2025). Early and opposing neutrophil and CD4 T
601 cell responses shape pulmonary tuberculosis pathology. J Exp Med *222*, e20250161.
602 https://doi.org/10.1084/jem.20250161.

603 50. Mai, D., Jahn, A., Murray, T., Morikubo, M., Lim, P.N., Cervantes, M.M., Pham, L.K., Nemeth,
604 J., Urdahl, K., Diercks, A.H., et al. (2024). Exposure to Mycobacterium remodels alveolar
605 macrophages and the early innate response to Mycobacterium tuberculosis infection. PLoS
606 Pathog *20*, e1011871. https://doi.org/10.1371/journal.ppat.1011871.

607 51. Chin, J., Abeydeera, N., Repasy, T., Rivera-Lugo, R., Mitchell, G., Nguyen, V.Q., Zheng, W.,
608 Richards, A., Stevenson, E., Swaney, D.L., et al. (2025). Mycobacterium tuberculosis triggers
609 reduced inflammatory cytokine responses and virulence in mice lacking Tax1bp1. PLoS
610 Pathog *21*, e1012829. https://doi.org/10.1371/journal.ppat.1012829.

611 52. Pyle, C.J., Wang, L., Beerman, R.W., Jain, V., Ohman, H.K.E., Thompson, B.A., Abramson,
612 K.R., Ko, D.C., Gregory, S.G., Smith, C.M., et al. (2025). Paired single-cell and spatial
613 transcriptional profiling reveals a central osteopontin macrophage response mediating
614 tuberculous granuloma formation. mBio *16*, e0155925. https://doi.org/10.1128/mbio.01559-
615 25.

616 53. Wang, L., Ma, H., Wen, Z., Niu, L., Chen, X., Liu, H., Zhang, S., Xu, J., Zhu, Y., Li, H., et al.
617 (2023). Single-cell RNA-sequencing reveals heterogeneity and intercellular crosstalk in
618 human tuberculosis lung. J Infect *87*, 373–384. https://doi.org/10.1016/j.jinf.2023.09.004.

619 54. Mbano, I.M., Liu, N., Wadsworth, M.H., Chambers, M.J., Mpotje, T., Asowata, O.E., Nyquist,
620 S.K., Nargan, K., Ramsuran, D., Karim, F., et al. (2026). Single-cell and spatial profiling
621 highlights TB-induced myofibroblasts as drivers of lung pathology. J Exp Med *223*,
622 e20251067. https://doi.org/10.1084/jem.20251067.

623 55. Cai, X., Zheng, W., Shi, X., Chen, L., Liu, Z., and Li, Z. (2018). HBx-Derived Constrained
624 Peptides Inhibit the Secretion of Hepatitis B Virus Antigens. Mol Pharm *15*, 5646–5652.
625 https://doi.org/10.1021/acs.molpharmaceut.8b00807.

56. Cai, X., Padilla, N.T., Rosbe, K., and Tugizov, S.M. (2024). Breast milk induces the differentiation of monocytes into macrophages, promoting human cytomegalovirus infection. J Virol *98*, e0117724. https://doi.org/10.1128/jvi.01177-24.

57. Srivastava, S., Grace, P.S., and Ernst, J.D. (2016). Antigen Export Reduces Antigen Presentation and Limits T Cell Control of M. tuberculosis. Cell Host Microbe *19*, 44–54. https://doi.org/10.1016/j.chom.2015.12.003.

Acknowledgments

We thank Lucas Chen, Michael Kwon, and Kelley Martinez for technical assistance. This work was supported by NIH grants R01 AI051242 (J.D.E.), U01 AI166309 (J.D.E.), P30 AI168440/R25 AI147375 (W.Z. and A.M.), T32 HL007185 (A.M.), F32 HL162424 (A.M.), and F31 AI172360 (Z.P.H.). The funders had no role in study design, data collection, interpretation, or the decision to submit the work for publication.

Author contributions

Conceptualization, W.Z. and J.D.E.; methodology, W.Z., J.D.L., and Z.P.H.; investigation, W.Z., J.L., Z.P.H., and A.M.; resources: E.T.; writing—original draft, W.Z. and J.D.E.; writing—review & editing, W.Z. and J.D.E.; funding acquisition, W.Z., Z.P.H., A.M., and J.D.E.; supervision, W.Z. and J.D.E.

Declaration of interests

The authors declare no competing interests.

650 **Figure legends**

651

652 **Figure 1. Key proteins in IFNγ signaling pathway are expressed at lower levels in MNC1.**

653 (A) Analysis of RNA-seq dataset GSE288567 revealed that IFNγ signature genes are expressed
654 at lower levels in CD11c^{lo} monocyte-derived cells (MNC1) compared with alveolar macrophages
655 (AM) and CD11c^{hi} MNC2 (28 dpi). 10,000 live cells from each subset were sorted from the lungs
656 of C57BL/6 mice infected with Mtb H37Rv-mCherry (n = 7-8).

657 (B) A schematic diagram shows the key signaling proteins regulating the response to IFNγ and
658 representative IFNγ-responsive genes.

659 (C) Messenger RNAs encoding key signaling proteins regulating the response to IFNγ and
660 representative IFNγ-responsive genes are differentially expressed in AM, MNC1, and MNC2.
661 Shown are mRNA normalized read counts for different cell subsets (28 dpi) (n=7-8).

662 (D) Key signaling proteins regulating the response to IFNγ and protein products of representative
663 IFNγ-responsive genes are differentially expressed in AM, MNC1, and MNC2. Flow cytometry
664 was used to measure median fluorescent intensity (MFI) of proteins in different lung cell subsets
665 from mice infected with H37Rv-ZsGreen. Fold change values were for AM vs. MNC1, MNC2 vs.
666 MNC1, and AM vs. MNC2 (n=4-5).

667 Results are presented as mean ± SD. *p<0.05, **p<0.01, ***p<0.0001, ****p<0.0001 by Wald test
668 via DESeq2 for (C) and one-way ANOVA with Tukey's multiple comparison test for (D); ns = not
669 significant.

670

671

672 **Figure 2. STAT1 phosphorylation is deficient in MNC1 treated with IFNγ ex vivo.**

673 (A) Workflow for detecting pSTAT1 by flow cytometry and immunofluorescence. C57BL/6 mice
674 were infected with Mtb H37Rv-ZsGreen via aerosol for 28 days. Lung single-cell suspensions
675 were incubated with 20 ng/mL IFNγ for 15 min and subjected to pSTAT1 by flow cytometry
676 analysis or immunofluorescence.

677 (B) MFI of pSTAT1 by flow cytometry for each lung cell subset in the absence or presence of IFNγ
678 stimulation as described in panel A. Fold change values were for AM vs. MNC1, MNC2 vs. MNC1,
679 and AM vs. MNC2 (n=6).

680 (C) Fold change of pSTAT1 MFI level by flow cytometry after cells were stimulated with IFNγ ex
681 vivo as described in panel B (n=6).

682 (D) Representative images of nuclear pSTAT1 immunofluorescence staining for each cell subset
683 sorted from Mtb-infected mice (28 dpi). Bottom panel shows the quantitation of mean fluorescence
684 intensity of nuclear pSTAT1 from n>145 cells.

685 (E) Representative images of nuclear pSTAT1 immunofluorescence staining for each cell subset
686 sorted from Mtb-infected mice (28 dpi) and stimulated with 20 ng/mL IFNγ for 15 min. The bottom
687 panel shows the quantitation of the mean fluorescence intensity of nuclear pSTAT1 from >155
688 cells. Fold change values were for AM vs. MNC1, MNC2 vs. MNC1, and AM vs. MNC2.

689 (F) Fold change of nuclear pSTAT1 MFI by immunofluorescence staining after cells were
690 stimulated with IFNγ ex vivo as described in panel E.

691 Results are presented as mean ± SD. Brown-Forsythe and Welch ANOVA tests with
692 Dunnett's T3 multiple comparisons test (B, D-F) and One-way ANOVA with Tukey's multiple
693 comparison test (C) were used to determine statistical significance. ***p<0.001, ****p<0.0001 by
694 one-way ANOVA; ns = not significant.

695

696

697 **Figure 3. Impaired responsiveness to IFNγ in MNC1 associates with defective MHC-II**
698 **antigen presentation.**

699 (A) Heatmap of the Z-scores from variance-stabilized read counts for genes related to MHC-II
700 antigen presentation (adjusted p-value ≤ 0.05 and |log2 fold change|>0.5).

701 (B-C) MNC1 express less surface MHC-II (B) and CD74 (C) than AM and MNC2. Flow cytometry
702 was used to measure MFI of MHC-II and CD74 in each cell subset from mice infected with Mtb
703 H37Rv-ZsGreen (28 dpi). Fold change values were for AM vs. MNC1, MNC2 vs. MNC1, and AM
704 vs. MNC2 (n=5).

705 (D) Workflow of antigen-specific T cells and lung mononuclear phagocyte co-culture. $1x10^4$ cells
706 were sorted from mice infected with Mtb H37Rv-ZsGreen and incubated with $2x10^5$ of the
707 indicated Th1 polarized TCR transgenic antigen-specific T cells and 10ug/mL antigenic peptide.
708 After 24h, the supernatant was filtered and assayed for IFNγ using ELISA.

709 (E-F) Impaired antigen presentation to CD4 T cells by MNC1. Supernatants were harvested from
710 the co-culture of antigen-specific T cells and different sorted cell subsets, and IFNγ level was
711 measured by ELISA. Fold change values were for AM vs. MNC1, MNC2 vs. MNC1, and AM vs.
712 MNC2 (n=4).

713 Results are presented as mean ± SD. One-way ANOVA with Tukey's multiple comparison test
714 (B) and Brown-Forsythe and Welch ANOVA tests with Dunnett's T3 multiple comparisons test (C,
715 E-F) were used to determine statistical significance. *p<0.05, **p<0.01, ****p<0.0001; ns = not
716 significant.

717

718

719 **Figure 4. Type I IFN contributes to defective IFNγ responses and MHC-II expression in**
720 **BMDM and MNP subsets.**

721 (A) Heatmap of the Z-scores from variance-stabilized read counts for IFNβ signature genes

722 (adjusted p-value ≤ 0.05 and |log2 fold change|>0.5, n=7-8).

723 (B-C) Type I IFN suppresses MHC-II expression induced by IFNγ in vitro. Wild-type (WT) or *Ifnar1*$^{-}$
724 $^{/-}$ bone marrow cells were differentiated in bone marrow-derived macrophage (BMDM) media
725 containing the indicated interferon at 50 pg/mL for 6-7 days. The expression levels of MHC-II in
726 BMDM were determined by flow cytometry and expressed as median fluorescence intensity (MFI)
727 (n=4).

728 (D) Experimental workflow. CD45.1/45.2 mice were irradiated and reconstituted with 1:1 mixed
729 bone marrow from WT CD45.1/45.2 mice and *Ifnar1*$^{-/-}$ CD45.2/45.2 mice. After 6-week
730 reconstitution, chimeras were aerosol challenged with Mtb H37Rv-ZsGreen.

731 (E) Type I IFN regulates MHC-II expression in AM, MNC1, and MNC2 in vivo. Flow cytometry was
732 used to measure MHC-II MFI in each subset from WT: *Ifnar1*$^{-/-}$ mixed bone marrow chimeric mice
733 infected with Mtb H37Rv-ZsGreen for 28 days (n=4).

734 Results are presented as mean ± SD. *p<0.05, **p<0.01, ***p<0.0001, ****p<0.0001 by one-way
735 ANOVA with Tukey's multiple comparison test for (B-C) or by paired t-test for (E); ns = not
736 significant.

737

738

739 **Figure 5. CoMtb improves IFNγ responsiveness of MNC but not AM.**

740 (A) For the contained Mtb (CoMtb) studies, mice were inoculated intradermally in the ear with
741 10,000 CFU of Mtb H37Rv. After 4-6 weeks, control and CoMtb mice were infected with Mtb
742 H37Rv-ZsGreen by aerosol and euthanized at 28 dpi.

743 (B) CoMtb increases IFNγ responsiveness in bone marrow monocytes. Bone marrow cells from
744 control or coMtb mice were stimulated with or without 20 ng/mL IFNγ for 15 min, followed by flow
745 cytometric measurement of pSTAT1 MFI (n=3).

746 (C) CoMtb increases IFNγ responsiveness in BMDM. Bone marrow cells from control or coMtb
747 mice were differentiated into BMDM for 6 days. Then BMDM were harvested and stimulated with
748 or without 20 ng/mL IFNγ for 15 min, followed by flow cytometric measurement of pSTAT1 MFI
749 (n=3).

750 (D) CoMtb improves IFNγ responsiveness in MNC1 and MNC2. Lung samples from control or
751 coMtb mice infected with H37Rv-ZsGreen by aerosol (28 dpi) were stimulated with or without 20
752 ng/mL IFNγ for 15 min, followed by flow cytometric measurement of pSTAT1 MFI (n=5-6).

753 (E) CoMtb increases expression of IFNGR2 in MNC1 and MNC2. Shown are IFNGR2 MFI by flow
754 cytometry for each lung cell subset from control or coMtb mice infected with H37Rv-ZsGreen by
755 aerosol (28 dpi) (n=5-6).

756 (F) CoMtb enhances MHC-II expression in MNC1 and MNC2. MHC-II MFI was measured by flow
757 cytometry (28 dpi) (n=4-5).

758 (G) MNC1 and MNC2 from CoMtb mice show a higher expression of NOS2 by flow cytometry (28
759 dpi) (n=4-5).

760 Results are presented as mean ± SD. *p<0.05, **p<0.01, ***p<0.0001, ****p<0.0001 by unpaired
761 t tests; ns = not significant.

762

763

764 **Figure 6. CoMtb-mediated prior immunity improves Mtb control in lung myeloid cells.**

765 (A) Total lung CFU for control or CoMtb mice infected with Mtb H37Rv-ZsGreen via aerosol for
766 28 days (n=5).

767 (B) The number of total live infected cells from the same lung in panel A (n=5).

768 (C) Bacterial burden indicated by ZsGreen MFI by flow cytometry for total infected cells in panel
769 B (n=5).

770 (D) Number of infected cells in each subset from the lungs of control and CoMtb mice infected
771 with Mtb H37Rv-ZsGreen via aerosol for 28 days (n=5-6).

772 (E) Frequency of Mtb-infected cells in each lung subset from control and CoMtb mice infected
773 with Mtb H37Rv-ZsGreen via aerosol for 28 days (n=5).

774 (F) Bacterial burden in each infected lung cell subset from control and CoMtb mice infected with
775 Mtb H37Rv-ZsGreen via aerosol for 28 days (n=5).

776 (G) Irradiated mice received 5 x 10^6 T cell-depleted bone marrow cells from control or coMtb mice.
777 After reconstitution for 8 weeks, mice were infected with aerosol Mtb for 28 days.

778 (H) Lung Mtb burden for Mtb-infected chimeric mice that received bone marrow cells from control
779 or coMtb mice (28 dpi) (n=3-4).

780 (I) To generate mixed bone marrow chimeric mice, recipient (CD45.1/45.1) mice were irradiated
781 and reconstituted with 1:1 mixed bone marrow from WT mice and *Ifngr1*$^{-/-}$ CD45.2/45.2 mice for 8
782 weeks. After 4 weeks of CoMtb, mice were aerosol challenged with Mtb H37Rv-ZsGreen.

783 (J) Bacterial burden indicated by ZsGreen MFI in infected AM and MNC cells from infected bone
784 marrow chimeric mice. There were insufficient infected MNC1 in CoMtb mice for separate
785 analyses, so MNC1 and MNC2 were combined as MNC in these studies (n=6).

786 (K) Ratio of *Ifngr1*$^{-/-}$/WT Mtb burden in different Mtb-infected subsets (ZsGreen^{+}) from infected
787 bone marrow chimeric mice (n=6).

788 Results are presented as mean ± SD. *p<0.05, **p<0.01, ***p<0.0001, ****p<0.0001 by unpaired
789 t-test (A-F, H), or by paired t-test for (J-K); ns = not significant.

790

791

792 **Figure 7. Proposed model of subset-specific IFNγ responsiveness in Mtb infection.**

793 In Primary infection, MNC1 exhibit low levels of IFNγ signaling components (e.g., IFNGR2). This
794 impaired responsiveness, compounded by Type I IFN-mediated suppression of MHC-II
795 expression, renders MNC1 cells highly permissive to intracellular Mtb growth and reduces their
796 ability to be activated by CD4 T cells. In contrast, MNC2 and AM maintain higher IFNγ
797 responsiveness. In CoMtb model, monocyte-derived cells undergo training, showing enhanced
798 IFNγ responsiveness and upregulated MHC-II expression. This shift results in a more robust
799 activated phenotype, leading to improved restriction of Mtb replication and superior protective
800 immunity. Created with biogdp.com.
801

802

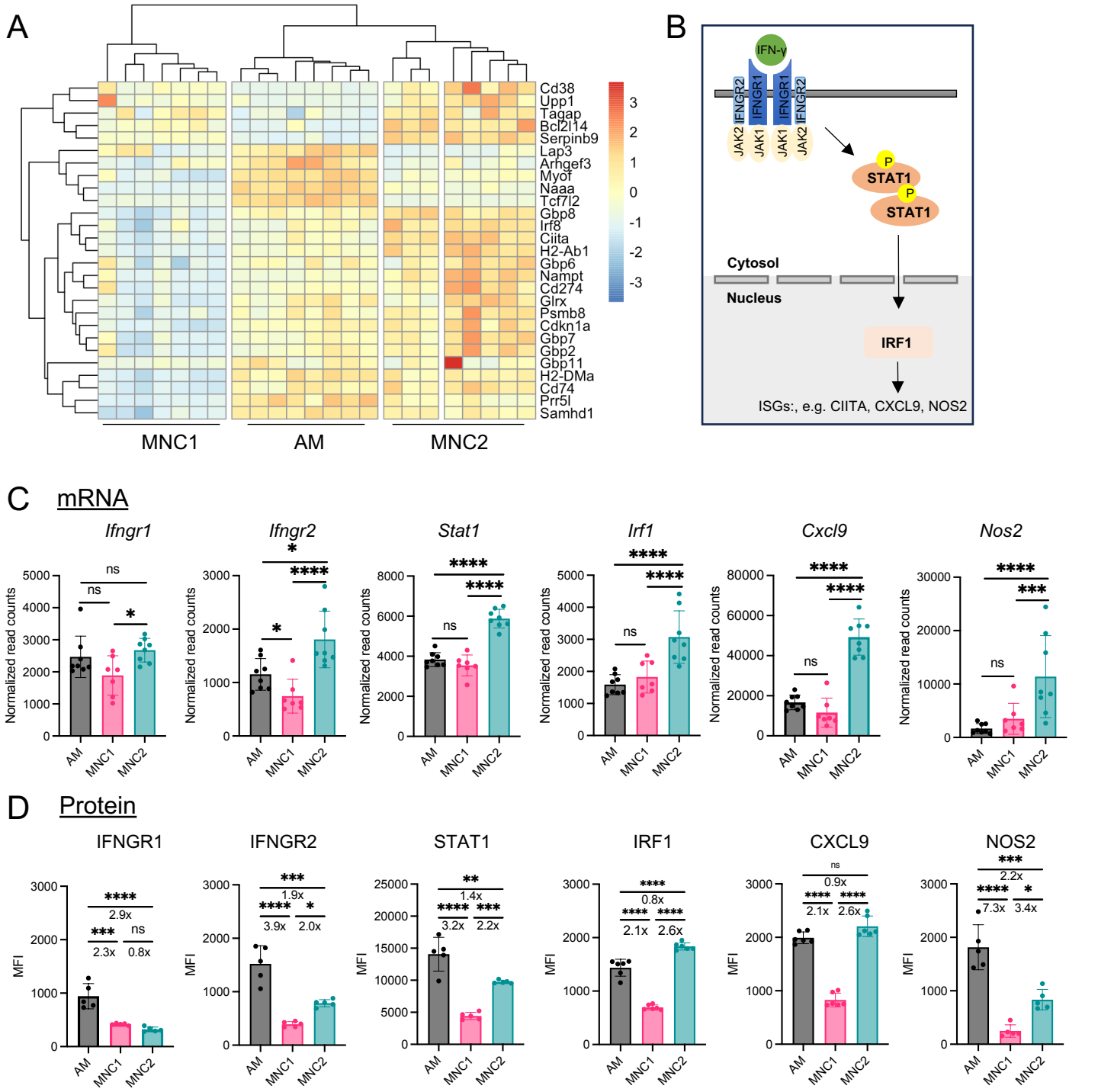
A
Cd38
Upp1
Tagap
Bcl2l14
Serpinb9
Lap3
Arhgef3
Myof
Naaa
Tcf7l2
Gbp8
Irf8
Ciita
H2-Ab1
Gbp6
Nampt
Cd274
Glrx
Psmb8
Cdkn1a
Gbp7
Gbp2
Gbp11
H2-DMa
Cd74
Prr5l
Samhd1
3
2
1
0
-1
-2
-3
MNC1
AM
MNC2
B
IFN-γ
IFNGR2
IFNGR1
IFNGR1
IFNGR2
JAK2
JAK1
JAK1
JAK2
P
STAT1
P
STAT1
Cytosol
Nucleus
IRF1
ISGs:, e.g. CIITA, CXCL9, NOS2
C
mRNA
Ifngr1
Ifngr2
Stat1
Irf1
Cxcl9
Nos2
Normalized read counts
AM
MNC1
MNC2
D
Protein
IFNGR1
IFNGR2
STAT1
IRF1
CXCL9
NOS2
MFI
2.9x
2.3x
0.8x
1.9x
3.9x
2.0x
1.4x
3.2x
2.2x
0.8x
2.1x
2.6x
0.9x
2.1x
2.6x
2.2x
7.3x
3.4x

Figure 1

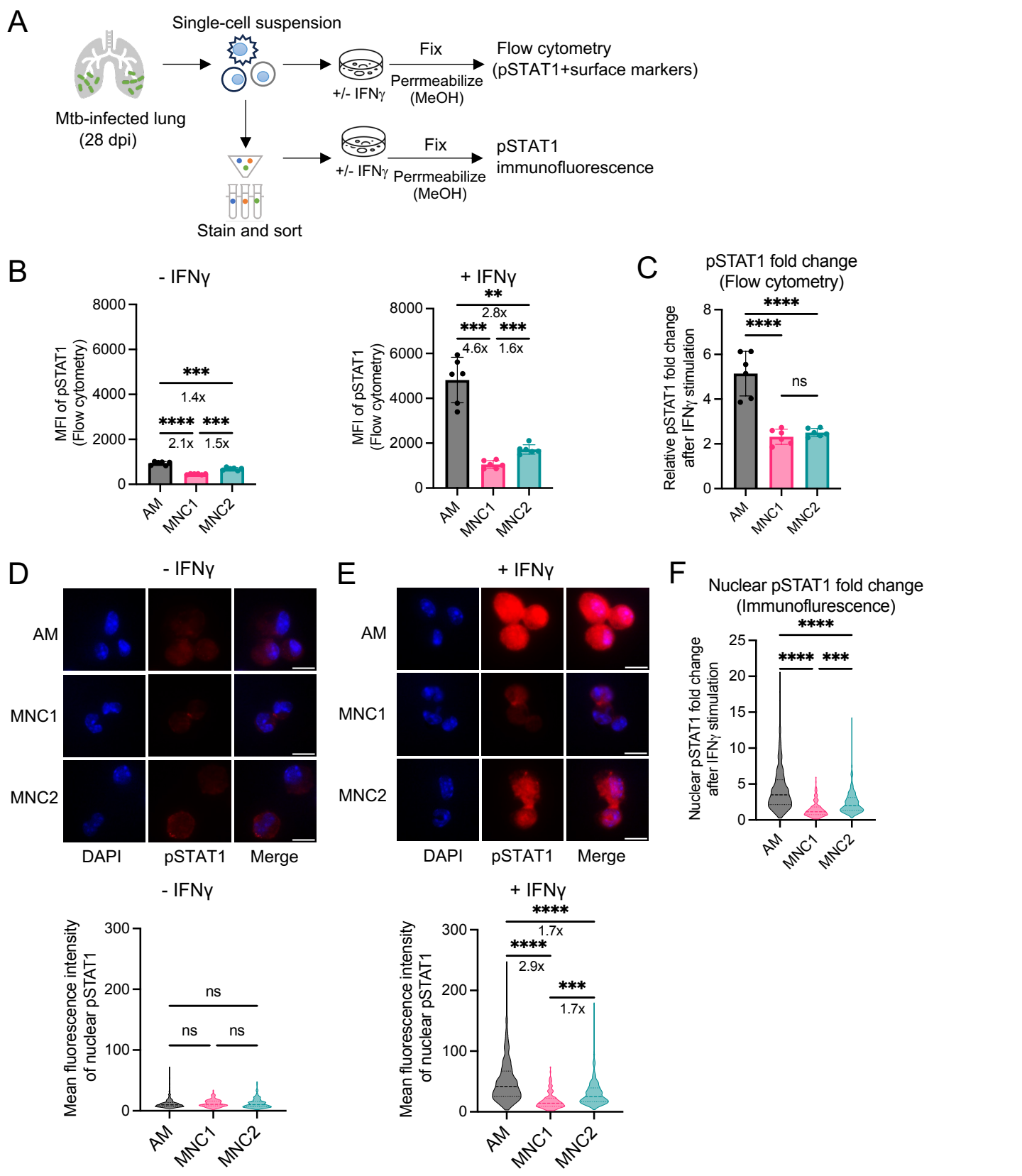
A
Single-cell suspension
Mtb-infected lung
(28 dpi)
+/- IFNγ
Fix
Perrmeabilize
(MeOH)
Flow cytometry
(pSTAT1+surface markers)
Stain and sort
pSTAT1
immunofluorescence
B
- IFNγ
+ IFNγ
MFI of pSTAT1
(Flow cytometry)
AM
MNC1
MNC2
C
pSTAT1 fold change
(Flow cytometry)
Relative pSTAT1 fold change
after IFNγ stimulation
ns
D
E
DAPI
pSTAT1
Merge
F
Nuclear pSTAT1 fold change
(Immunoflurescence)
Nuclear pSTAT1 fold change
after IFNγ stimulation
Mean fluorescence intensity
of nuclear pSTAT1

Figure 2

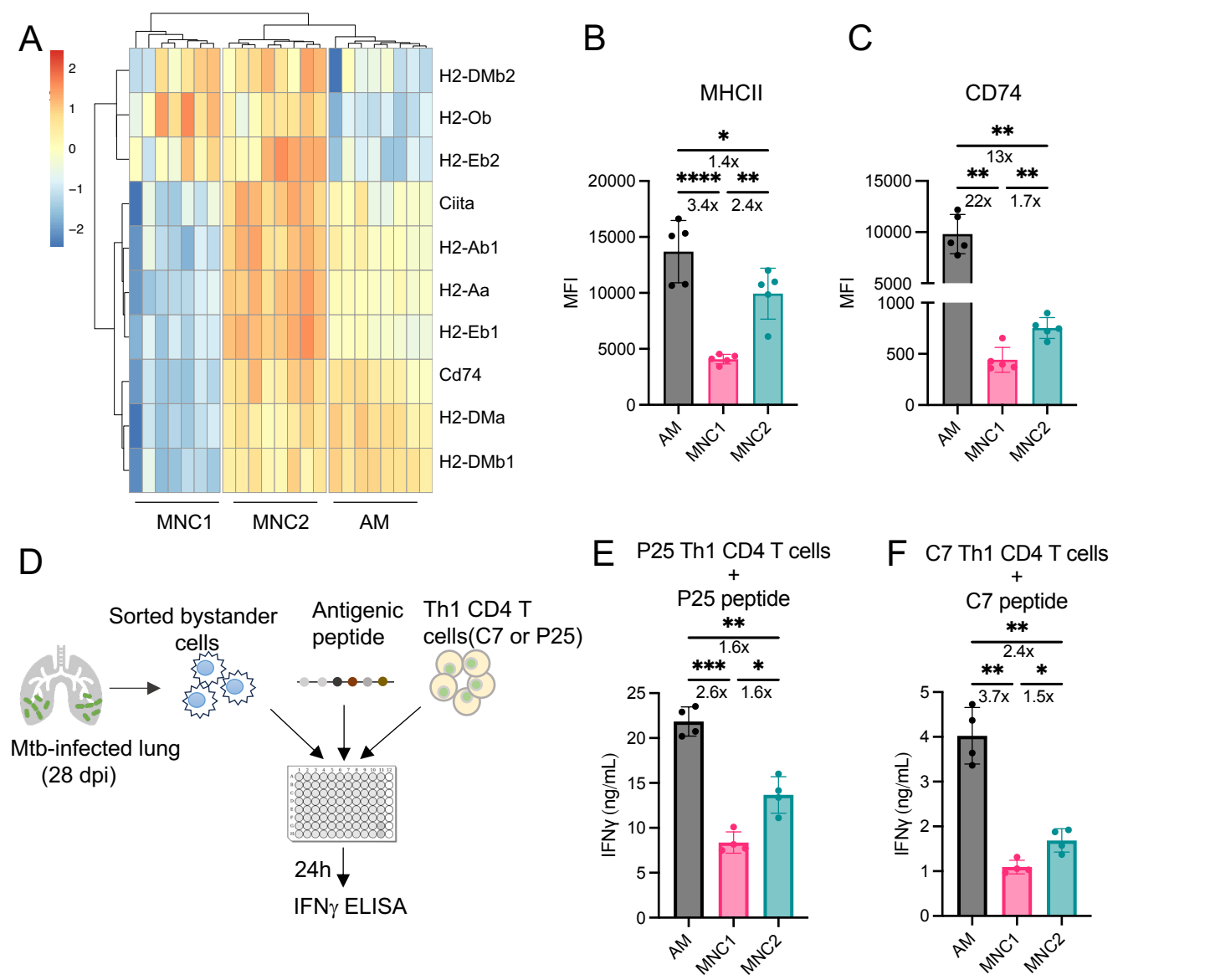
A
2
1
0
−1
−2
H2-DMb2
H2-Ob
H2-Eb2
Ciita
H2-Ab1
H2-Aa
H2-Eb1
Cd74
H2-DMa
H2-DMb1
MNC1
MNC2
AM
B
MHCII
MFI
20000
15000
10000
5000
0
*
1.4x
****
**
3.4x
2.4x
AM
MNC1
MNC2
C
CD74
MFI
15000
10000
5000
1000
500
0
**
13x
**
**
22x
1.7x
AM
MNC1
MNC2
D
Sorted bystander cells
Antigenic peptide
Th1 CD4 T cells(C7 or P25)
Mtb-infected lung (28 dpi)
24h
IFNγ ELISA
E
P25 Th1 CD4 T cells + P25 peptide
IFNγ (ng/mL)
25
20
15
10
5
0
**
1.6x
***
*
2.6x
1.6x
AM
MNC1
MNC2
F
C7 Th1 CD4 T cells + C7 peptide
IFNγ (ng/mL)
5
4
3
2
1
0
**
2.4x
**
*
3.7x
1.5x
AM
MNC1
MNC2

Figure 3

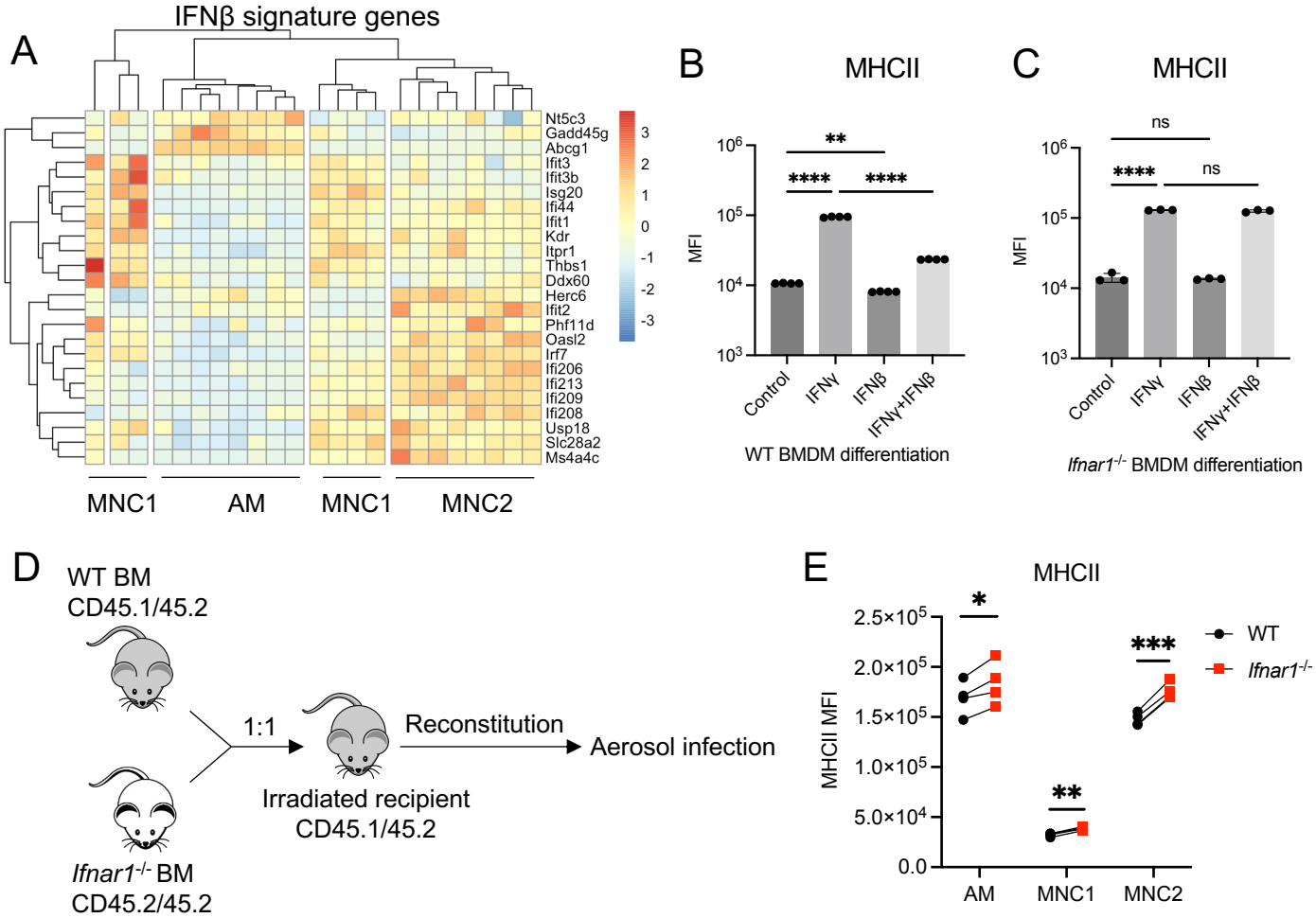
A
IFNβ signature genes
Nt5c3
Gadd45g
Abcg1
Ifit3
Ifit3b
Isg20
Ifi44
Ifit1
Kdr
Itpr1
Thbs1
Ddx60
Herc6
Ifit2
Phf11d
Oasl2
Irf7
Ifi206
Ifi213
Ifi209
Ifi208
Usp18
Slc28a2
Ms4a4c
3
2
1
0
-1
-2
-3
MNC1
AM
MNC1
MNC2
B
MHCII
MFI
Control
IFNγ
IFNβ
IFNγ+IFNβ
WT BMDM differentiation
C
MHCII
ns
ns
MFI
Control
IFNγ
IFNβ
IFNγ+IFNβ
Ifnar1-/- BMDM differentiation
D
WT BM
CD45.1/45.2
1:1
Irradiated recipient
CD45.1/45.2
Reconstitution
Aerosol infection
Ifnar1-/- BM
CD45.2/45.2
E
MHCII
MHCII MFI
WT
Ifnar1-/-
AM
MNC1
MNC2

Figure 4

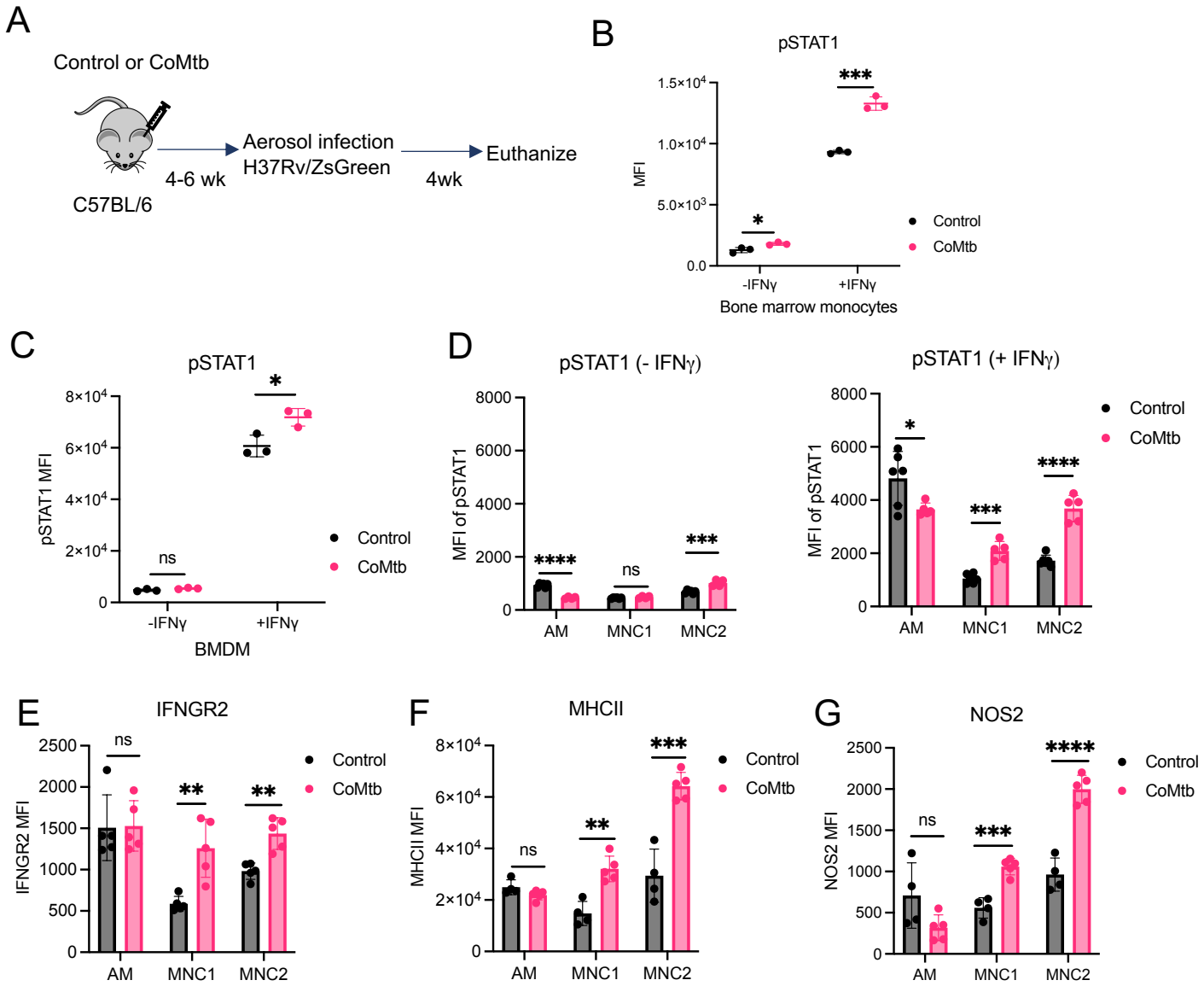
A
Control or CoMtb
C57BL/6
4-6 wk
Aerosol infection
H37Rv/ZsGreen
4wk
Euthanize
B
pSTAT1
MFI
1.5×10^4
1.0×10^4
5.0×10^3
0.0
***
*
-IFNγ
+IFNγ
Bone marrow monocytes
Control
CoMtb
C
pSTAT1
pSTAT1 MFI
8×10^4
6×10^4
4×10^4
2×10^4
0
ns
*
-IFNγ
+IFNγ
BMDM
Control
CoMtb
D
pSTAT1 (- IFNγ)
MFI of pSTAT1
8000
6000
4000
2000
0
****
ns
***
AM
MNC1
MNC2
pSTAT1 (+ IFNγ)
MFI of pSTAT1
*
***
****
Control
CoMtb
E
IFNGR2
IFNGR2 MFI
2500
2000
1500
1000
500
0
ns
**
**
AM
MNC1
MNC2
Control
CoMtb
F
MHCII
MHCII MFI
8×10^4
6×10^4
4×10^4
2×10^4
0
ns
**
***
AM
MNC1
MNC2
Control
CoMtb
G
NOS2
NOS2 MFI
2500
2000
1500
1000
500
0
ns
***
****
AM
MNC1
MNC2
Control
CoMtb

Figure 5

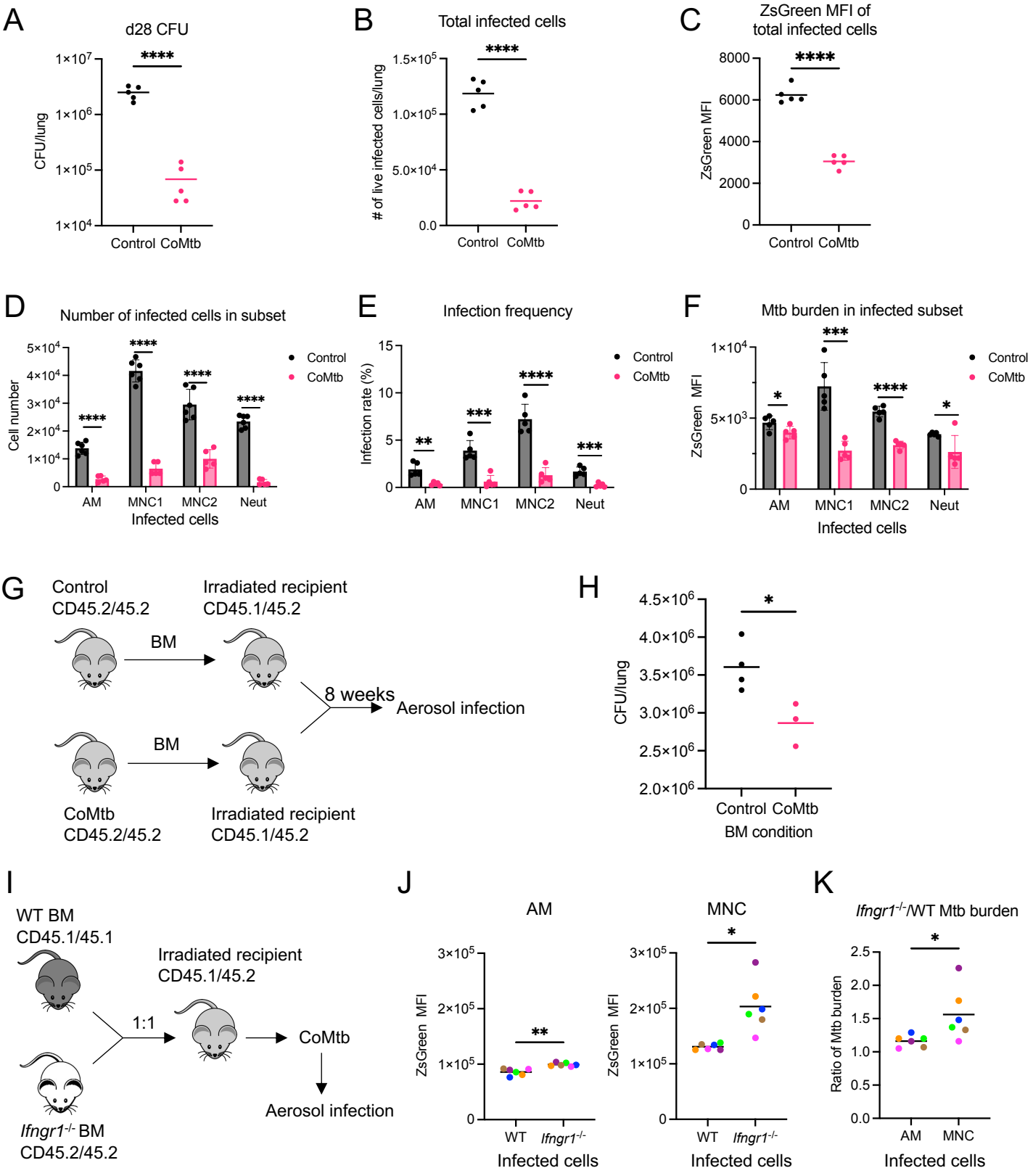
A
d28 CFU
CFU/lung
1×10^7
1×10^6
1×10^5
1×10^4
****
Control
CoMtb
B
Total infected cells
# of live infected cells/lung
1.5×10^5
1.0×10^5
5.0×10^4
0.0
****
Control
CoMtb
C
ZsGreen MFI of total infected cells
ZsGreen MFI
8000
6000
4000
2000
0
****
Control
CoMtb
D
Number of infected cells in subset
Cell number
5×10^4
4×10^4
3×10^4
2×10^4
1×10^4
0
****
****
****
****
AM
MNC1
MNC2
Neut
Infected cells
Control
CoMtb
E
Infection frequency
Infection rate (%)
15
10
5
0
**
***
****
***
AM
MNC1
MNC2
Neut
Control
CoMtb
F
Mtb burden in infected subset
ZsGreen MFI
1×10^4
5×10^3
0
*
***
****
*
AM
MNC1
MNC2
Neut
Infected cells
Control
CoMtb
G
Control
CD45.2/45.2
Irradiated recipient
CD45.1/45.2
BM
8 weeks
Aerosol infection
BM
CoMtb
CD45.2/45.2
Irradiated recipient
CD45.1/45.2
H
CFU/lung
4.5×10^6
4.0×10^6
3.5×10^6
3.0×10^6
2.5×10^6
2.0×10^6
*
Control
CoMtb
BM condition
I
WT BM
CD45.1/45.1
Irradiated recipient
CD45.1/45.2
1:1
CoMtb
Aerosol infection
Ifngr1-/- BM
CD45.2/45.2
J
AM
ZsGreen MFI
3×10^5
2×10^5
1×10^5
0
**
WT
Ifngr1-/-
Infected cells
MNC
ZsGreen MFI
3×10^5
2×10^5
1×10^5
0
*
WT
Ifngr1-/-
Infected cells
K
Ifngr1-/-/WT Mtb burden
Ratio of Mtb burden
2.5
2.0
1.5
1.0
0.5
0.0
*
AM
MNC
Infected cells

Figure 6

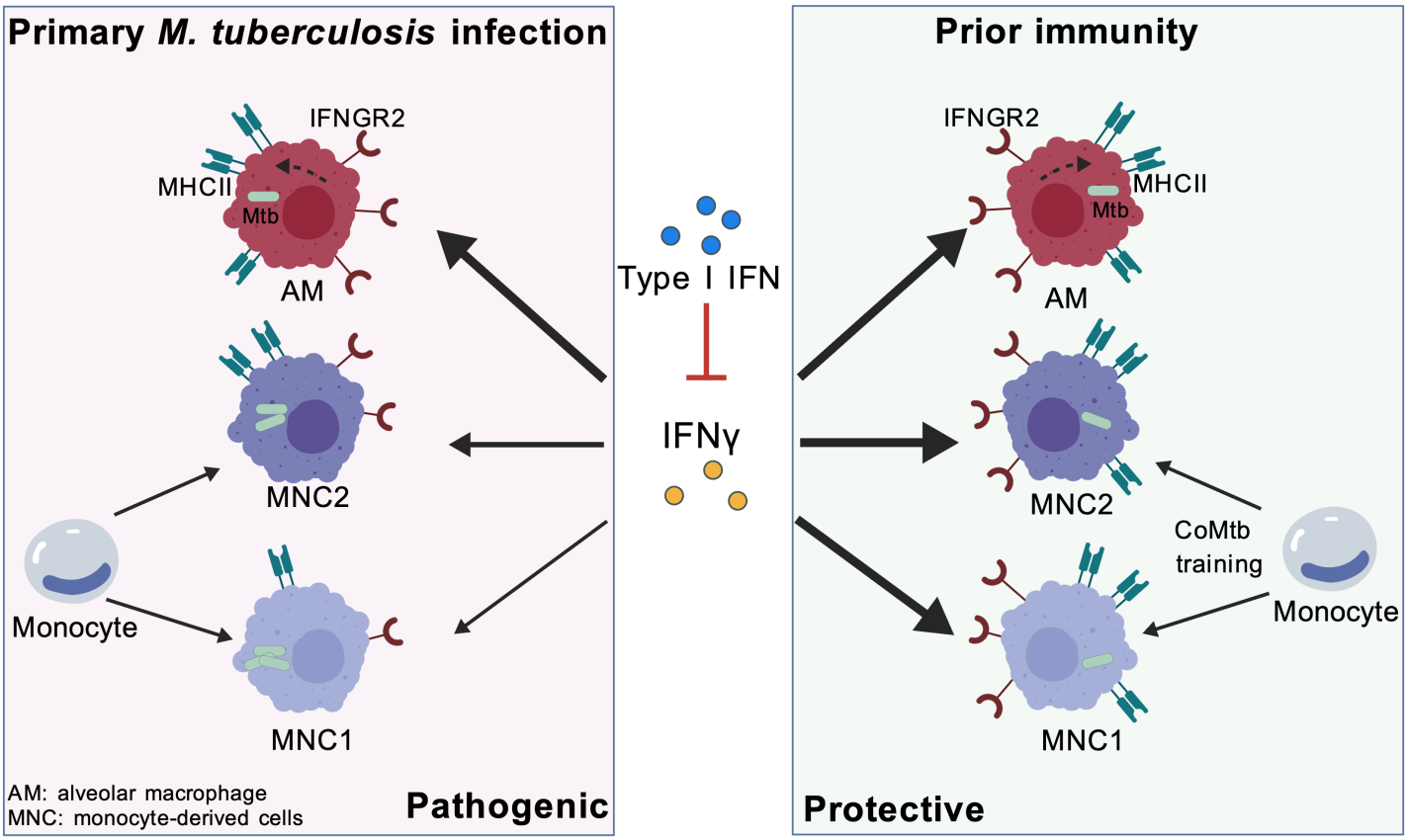
Primary *M. tuberculosis* infection
IFNGR2
MHCII
Mtb
AM
MNC2
Monocyte
MNC1
AM: alveolar macrophage
MNC: monocyte-derived cells
Pathogenic
Type I IFN
IFNγ
Prior immunity
IFNGR2
MHCII
Mtb
AM
MNC2
CoMtb
training
Monocyte
MNC1
Protective

Figure 7